Cracked Bearing Race Detection in Wind Turbine Gearboxes

C. Hatch
Principal Engineer/Technologist
charles.hatch@ge.com

A. Weiss
Engineering Manager, NPI
adam.weiss@ge.com

M. Kalb
Lead Engineer/Technologist
matt.kalb@ge.com

[Note: This article is based on a paper presented at the China Wind Power 2010 conference in Beijing, China in October 2010.]

Wind turbines are becoming established as an economically viable alternative to fossil-fueled power generation. Wind farms consisting of hundreds of units are now adding a significant amount to world generating capacity. As the size of wind farms continues to increase, business economics dictate careful asset management to minimize downtime and maximize availability and profits. A wind turbine condition monitoring system is essential to achieving that goal.

Wind turbine condition monitoring tends to focus on two primary groups of vibration frequencies: gear mesh frequencies and bearing defect frequencies. On typical 1.5 MW machines, the gearbox increases the input rotor speed of around 16 to 20 rpm to the generator speed of from 1400 to 1800 rpm. Most of these gearboxes have one planetary stage followed by two parallel stages. These stages typically produce three fundamental gear mesh frequencies (and their harmonics) that result from the meshing of a sun gear, planets, and a ring gear, plus two other pinions and gears.

Bearings in wind turbines are typically of rolling element design, and the gearbox contains five shafts supported by twelve or more bearings, each of which produces a set of five defect frequencies (outer race element pass, inner race element pass, cage or fundamental train, element spin, and twice element spin). It is easy to see that the combination of mesh frequencies, harmonics, and bearing defect frequencies can make frequency analysis a formidable task.

In addition, wind turbines are variable speed and power machines. Because of this, specific bearing and gearbox fault frequencies change with speed and must be carefully tracked. Variable power means variable torque and associated changes in gear meshing forces that can affect vibration amplitudes and mesh harmonic frequency content.

GE Energy has incorporated this knowledge into a new monitoring platform specifically designed for wind turbine condition-based monitoring, the Bently Nevada ADAPT.*wind monitoring system. The system includes a Bently Nevada 3701/60 monitor installed uptower in each wind turbine on the farm and a central farm server. The monitor uses an Ethernet connection to connect to the farm Supervisory Control And Data Acquisition (SCADA) network, which communicates to the farm server. The farm server is typically located at the farm central office, where it collects data from each 3701, and stores it in a local historian. ADAPT.wind software on the farm server is then used to view alarms and data collected from the monitors.

The ADAPT.wind platform automatically adjusts for wind turbine speed changes and extracts specific fault frequencies. To help compensate for the variable power and torque effects, the operating power range of the machine is divided into five bands, or modes, each with separate control over alarm levels. This allows more consistent comparison when trending data over long periods of time.

Recently, a number of new Bently Nevada 3701 ADAPT.wind monitoring systems were installed on a fleet of 1.5 MW wind turbines. These machines typically have three-stage increasing gearboxes: a planetary stage followed by two parallel stages. The 3701 system uses one accelerometer on the main bearing, three on the gearbox, and two more on the generator inboard and outboard (upwind and downwind) bearings. The three gearbox accels are mounted on the planetary ring gear, the high-speed intermediate shaft downwind bearing, and immediately adjacent to the high-speed output shaft downwind radial bearing. In addition, a two-axis accel is built into the 3701

for monitoring tower sway. The system can also utilize a Keyphasor* probe, mounted on the high-speed shaft to provide a speed reference. For bearing condition monitoring purposes, the 3701 monitors many vibration-based variables, including direct (overall) vibration amplitude, kurtosis, and crest factor; and it extracts timebase waveforms. It also tracks and extracts specific bearing fault frequency amplitudes from envelope spectra. The ADAPT.wind software has the capability to display trend plots, timebase waveforms, and both conventional and demodulated (enveloped) spectra.

In this case history, we will be discussing enveloped data from the gearbox high-speed shaft (HSS) accel (Figure 1). The diagnostic process utilized the high sensitivity provided by acceleration enveloping, so we will begin with a brief review of the enveloping process.

Bearing Faults and Acceleration Enveloping

Rolling element bearings usually fail by fatigue of the raceways or elements or, in generators, by electrostatic pitting of the raceways and elements. Another failure mode can involve cracking and fracture of the raceway. When a rolling element passes over a defect, the temporary loss of support causes the element to deflect slightly. When the element encounters the far side of the defect, the contact can usually produces a sharp impact to the bearing and support structure, similar to a car driving over a pothole in the road.

This impact causes a ringing of the bearing and support structure at the structural natural frequency. Each time an element encounters the defect, an impulse/response free vibration waveform is produced. The sequence of successive element passages produces a series of impulse/response events that repeat at the bearing defect frequency. If the defect is on an outer race, the events repeat at the outer race defect frequency; if the defect is on an inner race, the events repeat at the inner race defect frequency. Element faults produce defects related to the spin period of the element. All types of defects produce repeating series of impulse/response events that are visible in a timebase waveform.

Inner race faults have an additional characteristic. As the inner race rotates with the shaft, the defect moves from within the load zone of the bearing to outside the load

zone, where impacting is less likely to occur. This causes the amplitude of the impulse/response events to increase and decrease with each shaft rotation. It causes amplitude modulation of the impulse/response vibration, and the modulation pattern repeats at the shaft rotational frequency. This modulation is in addition to the defect modulation. Element faults can also produce additional modulation at the fundamental train, or cage, frequency as the damaged element moves into and out of the load zone. Because the outer race of a bearing is usually fixed, outer race faults do not produce this additional modulation.

Bearing defects produce a series of amplitude modulated impulses that are visible in a timebase waveform. This effect is analogous to an AM radio signal, where the content appears as changes in the amplitude (modulation) of a carrier signal. In AM radio, this carrier is around 1 MHz. In wind turbines, the carrier frequency is the structural natural frequency, which for typical machines is in the range of 4 to 10 kHz. Just as an AM radio signal carrier frequency is demodulated to extract the voice or music information, acceleration enveloping demodulates the high-frequency structural carrier frequency to extract the bearing fault repetition frequency.

When properly configured, acceleration enveloping will usually have a much higher sensitivity to faults that produce impacting. The structural natural frequencies "amplify" the vibration resulting from the impact and make them easier to detect.

Acceleration enveloping can be thought of as a four-step process: filter, rectify, envelope, and FFT. The filter band-pass region is set to include the range of structural natural frequencies (3701/60 monitor uses a 4-10 kHz bandpass filter for 1.5 MW turbines). The filtering removes rotor and gear mesh related vibration that could obscure the relatively small bearing fault signatures. After filtering, the signal is rectified, and an envelope is constructed that follows the extremes of the rectified signal fairly closely. The envelope typically has an approximately sawtooth wave shape, where a fast rise at the impulse is followed by a relatively slow decay. The envelope is then processed using a Fast Fourier Transform (FFT), producing a spectrum that is inspected for bearing fault frequencies. Note that the sawtooth envelope waveform shape will often produce a harmonic series based on the fundamental fault frequency. These harmonics are, typically, artifacts of the process and should be interpreted with caution. The fundamental fault frequency (and any sidebands) is usually the primary focus for bearing diagnostics. If an additional source of amplitude modulation is present (for example, an inner race defect where the impulse amplitude is modulated by rotor rotation frequency, or an element defect modulated by cage), an additional spectral line at this second modulation frequency will often be visible. We will see examples of this shortly.
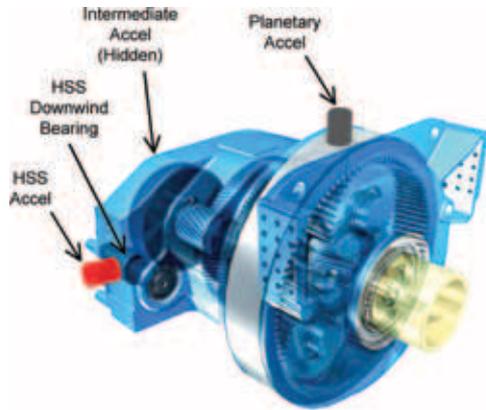
Figure 1: Wind turbine gearbox, viewed from the main rotor side. The high-speed shaft downwind bearing (HSS DW) and accel locations are shown. The high-speed accel location used for this case history is shown in red.
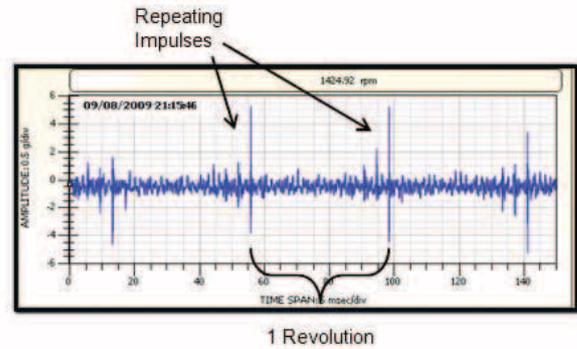
Figure 2: High-speed acceleration waveform from ADAPT.wind software showing periodic impulse patterns. The patterns repeat once every revolution.
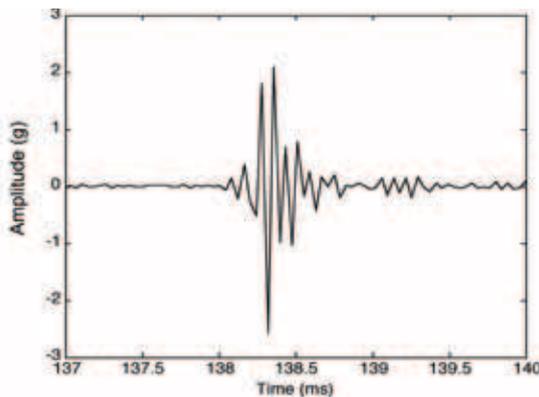
Figure 3: Zoom on a typical spike showing mechanical impulse/ response behavior.
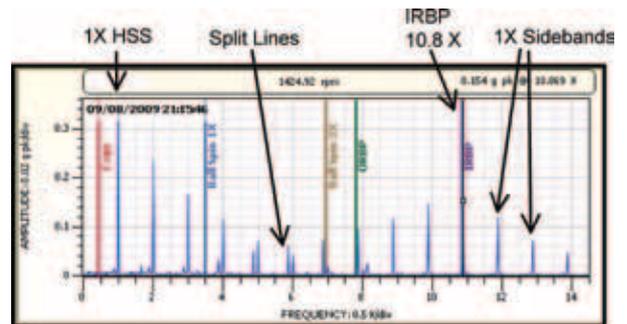
Figure 4: Acceleration envelope spectrum of waveform in Figure 2 (September 2009). The key bearing fault frequency lines are overlaid on the plot. The IRPB fault line is a perfect fit to the data. The split lines show that the two harmonic series are separated. Data processed in ADAPT.wind software.

Initial Detection

After deployment of the ADAPT.wind monitoring systems, some interesting vibration signatures were observed on a few gearboxes. On one, the timebase waveforms from the high-speed gearbox accelerometer showed a repeating pattern of symmetric impulses of very short duration (Figure 2). This waveform was captured in September 2009. The waveform shows a pattern of three impulses that increase and decrease in amplitude. As the inner race rotates through one revolution, the defect moves in an out of the radial load zone of the bearing, producing the long-wave modulation pattern. As it enters the load zone, the defect encounters successive rolling elements (cylindrical elements in this case). Each defect/element encounter produces an impulse in the waveform (the short period modulation pattern). The impulses increase in amplitude until a maximum is reached when

the defect is approximately aligned with the radial load direction in the bearing. Then, as the defect begins to leave the load zone, the impulses rapidly die away. This basic pattern is repeated once per revolution of the high-speed gearbox shaft and is highly suggestive of a single, inner-race defect in a bearing on that shaft.

Initially, the extremely narrow, sharp spike appearance in Figure 2 suggested an electrical noise problem on this accelerometer channel. To verify the data quality, several of the "spikes" in the signal were zoomed. Figure 3 shows a zoom from a similar waveform that has been exported and high-pass filtered at 5 kHz using MATLAB® software. The spike is clearly an impulse/response signature indicating mechanical vibration, not electrical noise. The vibration occurs at the "carrier" frequency that will be used for envelope demodulation. The enveloping bandpass filter was set from 4 kHz to 10 kHz, so this 5 kHz high-pass filtered plot shows approximately what the enveloping algorithm would see.

Enveloped spectra from this accelerometer display a rich harmonic series (Figure 4). This figure shows enveloped frequencies in orders of high-speed shaft (HSS) speed. The lowest fundamental corresponds to the HSS speed (1X HSS), and there are several harmonics. The next major feature is the inner-race ball pass (IRBP) frequency at 10.8X. This frequency agrees with the theoretical IRBP defect frequency for the high-speed downwind radial

bearing. A series of 1X sidebands are present on both sides of the central fault frequency line. (Most often, sidebands occur in spectra because of amplitude modulation of vibration happening at the center frequency.) The IRBP frequency at 10.8X is close to a harmonic of HSS speed at 11.0X, so at first glance, all the lines in the spectrum appear to be equally spaced harmonics of 1X. Close inspection shows that there really are two distinct harmonic series, one series based on 1X, and the other based on 1X sidebands from 10.8X. You can clearly see that the two families of spectral lines nearly overlap, and that separation is visible in the split lines near 5X and 6X.

The very rich spectrum occurs because of the extremely sharp impulses in the original waveform in Figure 2. The theoretical spectrum of a single, sharp, periodic impulse is an infinite harmonic series of narrow lines starting at the fundamental repeat frequency. In this case, we have a more complicated repetition pattern, but the sharp nature of the repeating impulses produce a similar effect in the envelope spectrum.

There are two sources of amplitude modulation in the waveform. The 10.8X line is obviously related to the inner race defect. This defect causes amplitude modulation of the waveform at the element pass period (the relatively small impulse spacing in Figure 2). The 1X line is caused by relatively large scale amplitude modulation as the inner race rotates in and out of the load zone. Both

sources of modulation are present, so both modulation frequency lines appear in the envelope spectrum, along with their harmonic series.

The monitor also calculates the kurtosis of the waveform. This is the fourth statistical moment of the waveform which emphasizes extreme values, so spikes in amplitude will tend to increase the kurtosis. The kurtosis of a pure sinusoidal waveform is 3. Because of the impulse/response behavior, the kurtosis of the waveform in Figure 2 is around 150.

Given the data so far, we concluded that a single defect existed on the HSS downwind radial bearing inner race. The extreme narrowness of the impulse/response signatures led us to suspect that the defect was a crack in the inner race; we reasoned that a broader spall would likely have produced a less well-defined impact signature. But at this time, because the overall amplitude of vibration was only 5 g, we recommended that the operator wait and watch. This would allow us to see how quickly the damage evolved. If it increased significantly, we would recommend shutting down the turbine.

More Data Arrives

For a few months after initial detection, the vibration signature remained relatively unchanged. However, when we looked again in April 2010, the vibration waveform had become more complex (Figure 5).
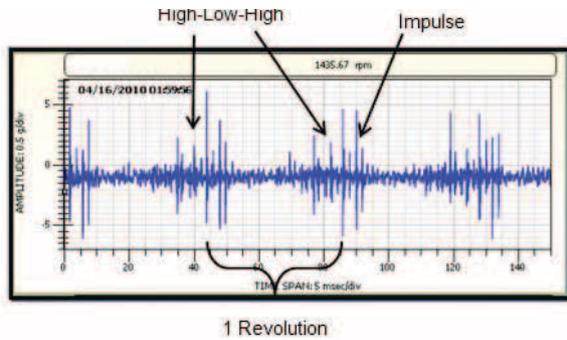
Figure 5: Data from the same bearing as Figure 2, but several months later. The vibration signature has become more complex.
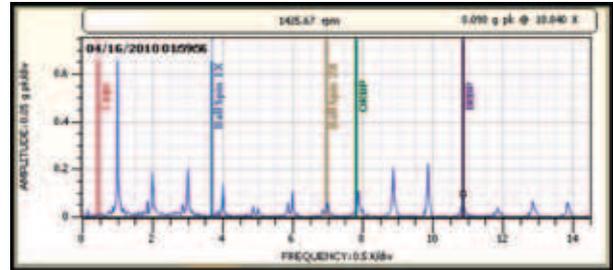
Figure 6: Data from April 2010. Compare to Figure 4. The amplitude of the IRBP line is lower, while the 1X line amplitude is higher.
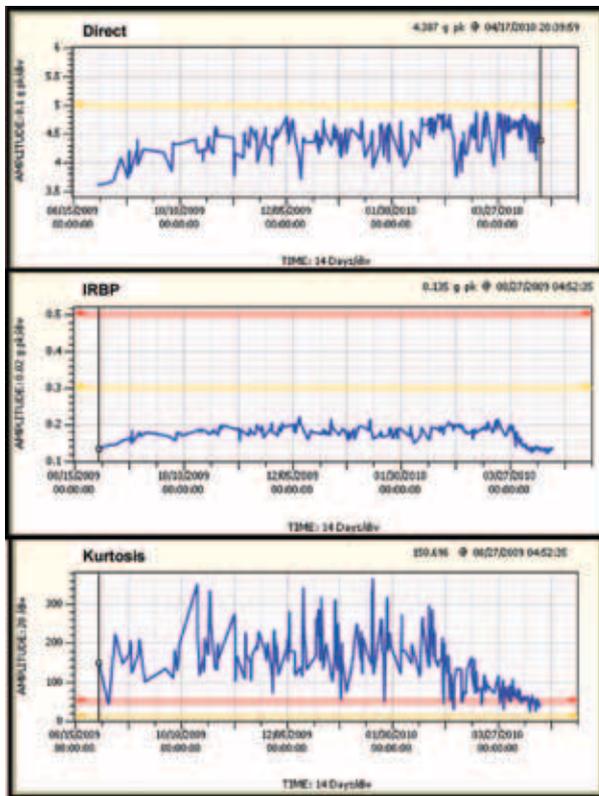
Figure 7: Trend plots from August 2009 to April 2010. Direct vibration (top) increases, but IRBP frequency amplitude (middle) and kurtosis (bottom) decrease near the end of the period.
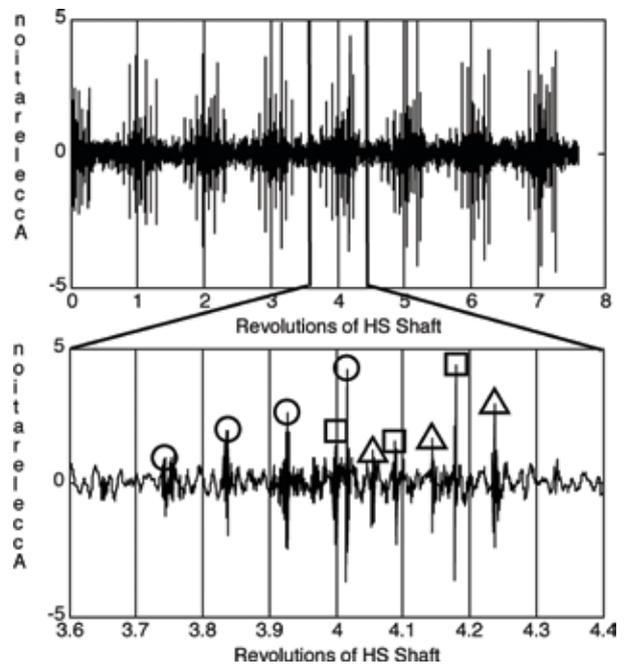
Figure 8: HSS accelerometer waveform from the second turbine gearbox. The circular, square, and triangular marks highlight three distinct patterns of fault induced impulses. This pattern suggests at least three separate inner race faults.

Although the amplitude of vibration remained about 5 g, there were two primary differences between the data in Figure 5 and the data in Figure 2. First, the impulse pattern in Figure 5 shows a repeating high-low-high impulse pattern with each revolution. This differs from the steadily rising amplitude pattern in Figure 2. Secondly, there is another set of lower-amplitude impulses that are offset by less than the element passage period from the larger set. This "double impulse" set appears at the same place every revolution. These changes suggest that more damage has developed on the inner race; the second change suggests that some of the additional damage is smaller than the original damage we observed before.

The envelope spectrum also shows some interesting changes. The 1X line has *increased* in amplitude, while the IRBP line has *decreased* (Figure 6, compare to Figure 4). The increase in 1X modulation has also increased the IRBP 1X sideband amplitude. This is interesting because it shows that more damage can actually reduce the IRBP amplitude.

Trends of direct vibration amplitude, IRBP amplitude, and kurtosis also changed over this period (Figure 7). Direct vibration slowly increases; this is a measure of the impulse amplitude we see in the timebase plots. The middle plot is the amplitude of the IRBP line in the envelope spectrum; it is approximately constant until it drops off near the end of the period. The kurtosis also declines near the end.

While the decline in IRBP is somewhat puzzling, the decline in kurtosis is caused by the larger number of impulse events in the waveform; in other words, the average signal excursion has increased. This reduces kurtosis, which is very sensitive to outliers. When everything is an outlier, then the outlier becomes the norm.

Figure 9: Crack in inner race of the high-speed downwind radial gearbox bearing (arrow). This was the largest of four race cracks found.

The impulse signatures still remained very narrow, and we suspected that a second crack had developed in the inner race. Still, at this time, overall vibration remained only about 5 g, so a decision was made to keep watching.

Another Turbine Exhibits Similar Behavior

In April 2010, another turbine was commissioned. This turbine was identical in every way to the first one. The HSS accelerometer data showed similar behavior to the first turbine (Figure 8, upper). This waveform shows a similar, very complex series of very narrow impulses.

The impulses appear to form three distinct repeating groups (these are marked in the lower figure with circles, squares, and triangles); in each group, impulses are separated by the IRBP fault period (1/10.8X = 0.093 revolutions) for the HSS downwind radial bearing. All of the impulses disappear and reappear once per revolution of the high-speed shaft. We concluded that at least three different faults on the inner race of the bearing were repeatedly passing through the bearing load zone. Note that the impulse amplitudes are also 4 to 5 g. Because there were so many indications of damage, we felt that there was a very good chance that this bearing would have visible damage that could confirm the diagnosis. This bearing is located in an accessible part of the gearbox, so the operator decided to replace this bearing, work that could be done up tower without a crane.

In May 2010 the bearing was replaced, and the original was inspected. We discovered four radial cracks in the inner race that extended some distance axially across a significant part of the race (Figure 9 shows the largest of them). None of these cracks had propagated all the way through the race, so there was some remaining useful life in the bearing.

Summary and Conclusions

The diagnosis of a cracked inner race was based on the following evidence:

- A clear pattern of modulated impulse/response signatures in the timebase waveform. This was consistent with an inner race bearing defect.

- IRBP bearing defect and 1X modulation frequency in the envelope spectrum. This confirmed the inner race fault, and the IRBP frequency identified the offending bearing.

- Very narrow impulse/response signatures in the timebase waveform suggested a narrow defect.

- A second, identical turbine exhibited similar symptoms on the same bearing. The bearing was removed and inspected, and four inner race cracks were found. Because of this confirmation, we are now confident that the original turbine has the same problem.

Trend plots of the first turbine data showed interesting behavior. While direct vibration increased at first and remained approximately constant, IRBP fault frequency and kurtosis amplitudes declined as damage progressed. These two measures appear to be most sensitive in the very early stages of bearing failure. Kurtosis is most sensitive when only one defect is present, as it is more of a statistical outlier. The reduction in IRBP amplitude may have been caused by an increased number of lower amplitude impulse events. This effect also caused an increase in the 1X modulation line amplitude in the spectrum. This shows the importance of using different kinds of data to monitor machine behavior. You cannot simply assume that all measures will increase with increasing damage!

In the first turbine, it took several months to evolve from a single defect to multiple defects, and given the bearing inspection results in the second turbine, there are probably at least several months more remaining life for this bearing. The bearing can remain in service, be monitored, and a convenient time can be scheduled for replacement.

The very close proximity of the sensor to the bearing probably made this diagnosis easier than it might have been if the transducer were mounted farther away. When farther, vibration propagation and reflection can muddy the impulse signatures in the timebase plot. Fortunately, the sensor was mounted close to the bearing, making this diagnosis more clear-cut. The diagnosis of these defects as cracks depended on both timebase and envelope spectrum information. Spectrum is, in one sense, an averaging process; the values displayed are average values over the entire waveform. Short-term time information is lost, and the timebase plot supplies that information, making the combination of the two plots more powerful than either one alone. The timebase plot also allows a cross check to check on the quality of the data.

This case has shown that it is possible to detect bearing race cracks at a very early stage, providing plenty of time to monitor and schedule maintenance. Timely warning is a key part of optimizing economic performance of a wind farm. ■

* denotes a trademark of Bently Nevada, Inc., a wholly owned subsidiary of General Electric Company.